New Compact and Broadband Patch Antenna Configurations for Wireless Applications

A. F. Almutairi, N. A. Aljuhaishi, and S. F. Mahmoud

EE Dept., Kuwait University, P.O. Box 5969, Safat, 13060, Kuwait
alialmut@eng.kuniv.edu.kw

Abstract – We present new compact patch antenna configurations with broadband capabilities for wireless applications. Analytical, simulation, and experimental work is performed on semi-circular and quarter-circular patch antennas with a shorting pin. The resonant frequencies and radiation fields of the dominant cavity modes of the shorted patch are derived. For the shorted semi-circular patch, the broadband operation is based on the efficient excitation of two staggered modes of the patch. It is shown that a relative bandwidth of 58% is achieved with a patch area that is only 13.6% of the central wavelength squared. The shorted quarter circular patch with the same radius as the half circular one provides a relative bandwidth of about 30%.

Keywords: Patch antennas, shorted patch, cavity modes, compact antennas, and wideband wireless communication.

I. INTRODUCTION

With the advancement of wireless communication services and networks, broadband operation and compact size have become essential parts of antenna design. Due to their many advantages, microstrip antennas are leading candidates for use in many fixed and portable wireless devices. Microstrip antennas are known for their low fabrication cost using printed circuit technology, light weight, low profile configuration, conformability to mounting host, and easy integration with microwave circuits on the same substrate [1-3]. Furthermore, they can easily produce linear polarization (LP) and circular polarization (CP) and they can be made in a compact form [4-6]. On the other hand, microstrip antennas suffer from some disadvantages such as low power handling capability. Therefore, they cannot be used in high power stages of radar and high power transmitters. However, they can be used in low power transmitters and wireless receivers in systems such as Bluetooth, Wi-Fi, Wi-Max, and ultrawideband (UWB).

Increasing the bandwidth of microstrip antennas has been an active and attractive research goal in the field of antenna's design. Efforts concentrating on broadening the bandwidth have been described in details in [7,8] and the references within. Reducing the size of microstrip antenna patch to be hosted in hand held wireless devices has also attracted many researchers lately. Effective ways of reducing the size of an antenna patch include patch loading by shorting posts [9,10] and/or introducing slots in the patch as has been detailed out in [11,12].

Microstrip patch antennas are widely designed to operate in the broad range of frequency from few hundreds of MHz to several GHz [8]. Several designs of microstrip antennas have been proposed in the literature to operate as multiband or broadband antennas. For example, a multiband H-shaped microstrip antenna designed to support modes with resonance frequencies at 2.2 GHz, 2.8 GHz, 3 GHz, and 5 GHz has been presented in [13]. Dual, triple, or quad band operations of the H-antenna were possible by the proper location of the coaxial feed in order to excite the required modes. An E-shaped wideband microstrip antenna design is proposed in [14] and a bandwidth of about 32.3% is achieved. The antenna is designed by incorporating two parallel slots into a square patch antenna to expand the bandwidth. In [15], a rectangular patch with a U-shaped slot is introduced as a broadband antenna with 27.5 % bandwidth referenced to the center frequency 1815 MHz. A compact polygonal patch antenna is achieved by designing a compact reactive ground plane made of a pattern of metallic patches [16]. A compact Y-shaped patch antenna that has two feeder ports and can be utilized in compact wireless devices to provide diversity signal or as a duplexer has been proposed in [17]. The effect of feed shape on the antenna bandwidth is studied in [18] where a rectangular microstrip antenna with an L-shaped probe is introduced. The L-shaped feed is shown to provide impedance matching over a broad band and a 28% bandwidth is reported. A modified bow-tie patch antenna has been introduced by Eldek et al [19] to operate in the wide band 5.5-12.5 GHz covering the C- and X bands. A circular microstrip patch antenna with a shorting post has been proposed and analyzed [20]. The authors show analytically that for a given operating frequency, a considerable reduction of patch size is possible by exciting the dominant mode. The analysis has been also extended to a 2-pin loaded circular patch [21], which can then operate as a dual or triple band antenna. The same

patch antenna can operate as a wideband antenna as shown in [22] where a bandwidth as high as 45% of the central frequency has been demonstrated.

In this paper, we propose a pin-loaded half and quarter circular patch antenna designs. In addition to their reduced patch size, these designs have wideband characteristics and can be used in many wireless devices. First, theory of the cavity modes of the pin loaded half circular patch is presented. The theoretical results lead to universal design curves for multiband or broadband operation of the antenna, so that an initial selection of the patch dimensions can be made. Simulations are then used to refine the design for a broadband operation. Simulation and experimental results are presented here to show the characteristics of the half and quarter circular patch antenna designs. As will be shown in the next section, compact and broadband performance is achieved by the proposed designs.

The rest of the paper is organized as follows: In section II, designs of broadband half and quarter circular patch antennas are outlined. In section III, computational results of selected antenna designs are presented. Experimental results for half and quarter circular antennas are shown, in section IV and concluding remarks are presented in section V.

II. ANALYSIS OF A SEMICIRCULAR PATCH ANTENNA

The purpose of this section is to find an analytical solution to the cavity modes on a half circular patch. As depicted in Fig. 1(a), a half circular patch of radius (a) lies on a grounded dielectric layer of thickness (h) and relative dielectric constant (ε_r). The patch is shorted at ($r=r_0$, $\phi=+\alpha$) by a shorting pin of radius (b) which is assumed much less than the patch radius. For an electrically thin substrate ($kh<<1$), the modal fields are independent of the z-coordinate so that the dominant modes are TM to z modes where E_z is the only nonzero component of the electric field. Adopting the cavity model for the patch, the planar boundary ($\phi = 0,\pi$) and the circular cylindrical boundary $r = a(0 \le \phi < \pi)$ are considered to behave as magnetic walls. To account for field fringing, we take (a) as an effective radius which is slightly greater than the physical radius and given by well known formulae [1].

Since the plane ($\phi = 0,\pi$) is considered as a magnetic wall, E_z being tangential to the plane will have a peak value on it. Hence, it is allowable to write $E_z(r,\phi)$ for a given cavity mode as,

$$E_z(r,\phi) = \sum_{n=0}^{\infty} A_n \cos(n\phi) J_n(kr) \exp(j\omega_r t) \quad (1)$$

for $0 \le r \le r_0$, and,

$$E_z(r,\phi) = \sum_{n=0}^{\infty} B_n \cos(n\phi)[J_n(kr)Y_n'(ka) - J_n'(ka)Y_n(kr)]\exp(j\omega_r t) \quad (2)$$

for $r_0 \le r \le a$, where ω_r is the cavity mode resonant frequency and $k = \omega_r\sqrt{\varepsilon_o \varepsilon_r \mu_o}$. The functions $J_n(x)$ and $Y_n(x)$ are the Bessel functions of first and second kind and the prime stands for differentiation with respect to the argument.

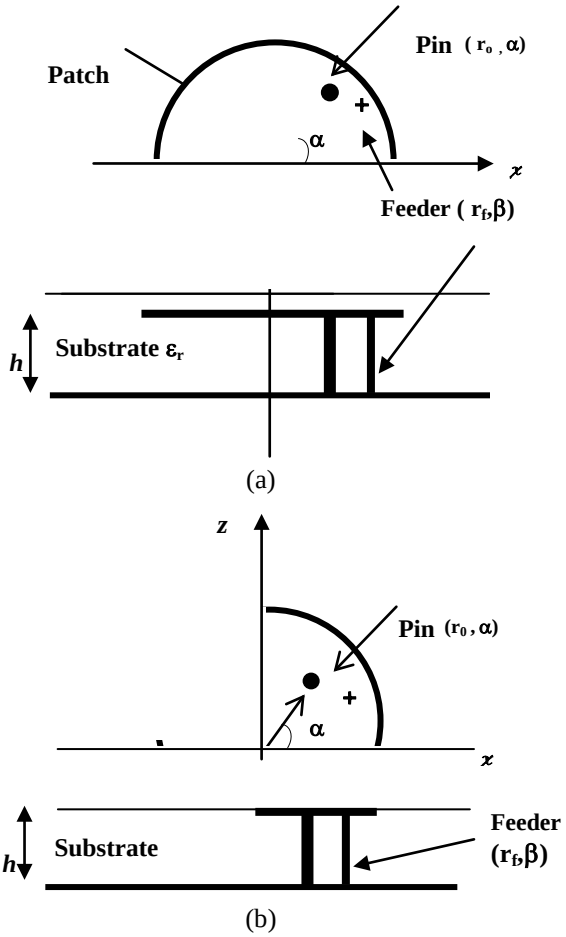

Fig. 1. Geometry of the proposed antennas composed of a half and quarter circular patch of radius "a" that is loaded by a pin and fed by a coaxial line. The pin of radius "b" is located at ($r_0, \alpha°$) and the feed position at (r_f, $\beta°$).

In equation (2), it is guaranteed that $\partial E_z / \partial r$ is equal to zero at $r = a$ which amounts to H_ϕ=0 on the magnetic wall. Next, we enforce the boundary condition at the pin position $r = r_0$. These conditions require the continuity of E_z across $r = r_0$ and the discontinuity of H_ϕ by the pin current. Enforcing these two boundary conditions, we get,

$A_n J_n(kr_o) =$

$$B_n [J_n(kr_o)Y_n'(ka) - J_n'(ka)Y_n(kr_o)], \quad (3)$$

$$H_\phi(r_o^+) - H_\phi(r_o^-) = \int_r J_z(r,\phi) r_o d \quad = I\delta(\phi-\alpha) \quad (4)$$

where $J_z(r,\phi)$ is the pin current density and '*I*' is the total pin current, assumed concentrated on its axis. since $H_\phi = \frac{-1}{j\omega\mu}\frac{\partial E_z}{\partial r}$, equation (4) leads to,

$$-\frac{1}{j\omega\mu}\{\sum_{n=0}^{\infty} B_n \cos(n\phi).k[J_n'(kr_o)Y_n'(ka) - J_n'(ka)Y_n'(kr_o)] - \sum_{n=0}^{\infty} A_n \cos n\phi.(kJ_n'(kr_o)\} =$$

$$I\delta(\phi-\alpha) = \frac{2I}{\pi}\sum_{n=0}^{\infty}\chi_n \cos n\phi.\cos n\alpha$$

where $\chi_n = 1$ for $n \geq 1$, and $\chi_0 = 1/2$ for $n = 0$.

Equating coefficient of $\cos n\phi$ on both side of the above equation, we get,

$$I\frac{2}{\pi}\chi_n \cos n\alpha = \frac{-k}{j\omega\mu}[B_n(J_n'(kr_o)Y_n'(ka) - J_n'(ka)Y_n'(kr_o))] + \frac{k}{j\omega\mu}[A_n J_n'(kr_o)] \quad (5)$$

using equations (2) and (5) , we get the coefficient A_n and B_n,

$$A_n = j\omega\mu I \chi_n \cos n\alpha \frac{J_n(kr_o)Y_n'(ka) - J_n'(ka)Y_n(kr_o)}{J_n'(ka)}$$

$$B_n = j\omega\mu I \chi_n \cos n\alpha \frac{J_n(kr_o)}{J_n'(ka)} \quad (6)$$

where we have used the Wronskian relation $J_n(x)Y_n'(x) - J_n'(x)Y_n(x) = 2/\pi x$.

Finally, the modal equation for the resonant frequency ω_r is obtained by imposing the boundary condition of vanishing E_z at the pin surface. Since the pin radius (*b*) is assumed very small relative to the field spatial variation, we are allowed to satisfy the vanishing of E_z at one line on the pin surface; say line ($r = r_0$-b, $\phi = \alpha$). So, using equation (1) and enforcing $E_z(r_o - b, \phi)$ to be zero, after some manipulations we get:

$$Y_o(kb) \pm Y_o(2kr_o \sin\alpha) - 4 \sum_{n=0}^{\infty}\chi_n \cos^2 \alpha [J_n(k(r_o-b)J_n(kr_o)]\frac{Y_n'(ka)}{J_n'(ka)} = 0 \quad (7)$$

which is the modal equation for the normalized resonant frequencies *ka*, where $ka = \omega_r \; a\sqrt{\varepsilon_r}/c$, with $\omega_r = \omega_{r1} = \omega_{r2}....$ being the modal resonant frequencies. The radiation fields of any particular cavity mode can be derived from the aperture E- field on the surface *r*=*a* as detailed in the Appendix.

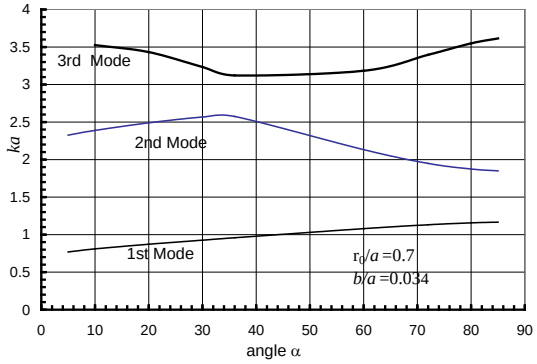

Fig. 2. Normalized resonant frequency *ka* for first 3 TM_n modes (in ascending order of *ka*) versus angle α. Here *b/a*=0.034 and r_0/a=0.7. *a* is the effective patch radius accounting for field fringing.

By solving the modal equation (7), we obtain Universal curves for the normalized resonant frequency ka of the first three modes as a function of the pin angular position 'α' for fixed r_0/a and b/a in Fig. 2. At this point, it is important to note that the field of any of these modes is a weighted sum of azimuthal harmonics (cos nϕ) of ϕ (see equations (1) and (2)). Thus one cannot identify modes as TM_{nm} where n indicates a fixed ϕ- harmonic in the usual way. Instead modes are identified as TM_m, m=1,2…., where each mode is characterized by a set of harmonic weights (A_n and B_n) as given by equation (6).

The lowest order mode TM_1 is the one having the lowest resonant frequency and therefore can provide a compact antenna design as demonstrated in [20] for the full circular patch with a shorting pin. For the parameters in Fig. 2, this mode resonates when *ka* is less than unity or $a \leq \lambda/2\pi$. However, operating in this mode will result in a narrowband operation [20]. Since in this paper we are interested in a broadband design, we will investigate this possibility by exciting the second and third order modes. This will be done in the next section.

III. BROADBAND SEMICIRCULAR PATCH ANTENNA DESIGN

Referring to Fig. 2, it is possible to achieve broadband operation of the semi-circular patch by

efficiently exciting the second and third order modes TM_2 and TM_3 and maintaining good matching between their resonant frequencies f_2 and f_3. This can be attained by a suitable choice of the feed position using the IE3D simulator as will be seen. Firstly we choose the patch radius '*a*' and the pin angular position α such as to place f_2 and f_3 within the frequency band of interest. The parameters r_0/a and b/a are fixed at their values in Fig. 2 although they can have other values.

To start a broadband design, we choose a patch radius of 35.38 mm on a substrate of relative permittivity (ε_r) = 2.2 and thickness = 6.28 mm. The effective patch radius, accounting for field fringing, is 39.39 mm. The pin has a radius (b) = 1.35 mm and is positioned at (r_0 , $+\alpha$) = (27.57,+ 60°). Using Fig. 2, these choices fix the frequencies of the second and third TM_2 and TM_3 modes at 1.95 GHz and 2.91 GHz respectively. Now we need to optimize the feed size and position in order to excite these modes and achieve matching over a broadband encompassing the range of frequencies f_2 to f_3. To this end, we have performed numerous simulations with varied feed positions on the IE3D software in order to maximize the bandwidth over which the input SWR is less than 2. These simulations are presented and discussed in the next section.

IV. Simulation Results for the Semi-Circular Patch

A. Standing Wave Ratio (SWR)

The Zealand IE3D software is used to simulate the semi-circular patch antenna using the patch and substrate parameters stated above. Numerous simulations are attempted with different feed radii and positions. It was concluded that broadband matching is achieved for a feed radius of 1.35 mm and radial position $r_f=r_0$. The angular position 'β' was found to be detrimental in realizing broadband matching. The simulation results for the standing wave ratio are plotted in Fig. 3 for $\beta = 0^0$, 5^0,10^0, 15^0 and 20^0. It is seen that the bandwidth, corresponding to SWR$\leq$2 depends on β. It is seen that maximum bandwidth occurs for $\beta = 10^0$. A summary of the results on percentage bandwidth and center frequency versus β are tabulated in Table 1. Here the center frequency is defined as the arithmetic mean of the upper and lower frequencies corresponding to SWR=2. The percentage bandwidth is maximum for $\beta = 10^0$ and equals 58 % around the center frequency 2.98 GHz (over the band 2.12-3.85 GHz). At this value of the feed angular position, the simulated complex input impedance is plotted against frequency in Fig. 4(a). The resistive component varies around 50 Ohms; between 30 to 100 Ohms over the band 2.1-3.9 GHz. Meanwhile the reactance oscillates slightly around zero Ohm. The Smith chart presentation of the complex impedance is given in Fig. 4(b). The circles around the center of the chart indicate a broadband operation.

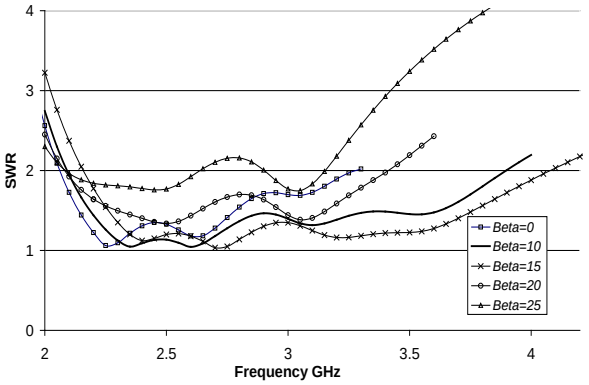

Fig. 3. SWR for a pin loaded semicircular patch with parameters (in mm): a = 35.38, h = 6.28, b = b_f = 1.35, r_o= r_f = 27.57, α=60 ° The feed angular position β = 0°, 10^0,15^0, and 20^0.

Table 1. Relative Bandwidth vs. Feed angular position.

	Angle β	Relative BW	@Center Frequency
1	0°	43%	2.61GHz
2	5°	56%	2.96GHz
3	10°	58%	2.98GHz
4	15°	56%	3.10GHz
5	20°	45%	2.71GHz

B. Directivity and Radiation Pattern

The simulated directivity and gain versus frequency are shown in Fig. 5 for the two representative cases of $\beta = 0^0$ and 10^0. It is seen that the directivity is quite flat with maximum deviation of ~0.5 dB around 8 dB over the band 1.6 GHz to 3.2 GHz for $\beta = 0^0$ and over the band 1.5 GHz to 4.0 GHz for $\beta = 10^0$. Thus, the antenna is not only broadband in terms of reflection loss, but also broadband in terms of directivity. On the other hand, the simulated gain varies over the bandwidth between 1 dB to 4.5 dB. This is less than the gain of the full circular patch of the same radius [21] which reaches a maximum of about 6 dB. This is not surprising and comes about as a consequence of size reduction.

The simulated two dimensional radiation patterns (or gain pattern) for $\beta = 10^0$ are given in Fig. 6(a) and (b) at the frequencies f=2.6 GHz and f=3.3 GHz. respectively. In these figures, the electric field components E_θ and E_ϕ are plotted in the E and H-planes. The radiation is mainly roadside and the crosspolar to copolar ratio is in the order of -8 dB.

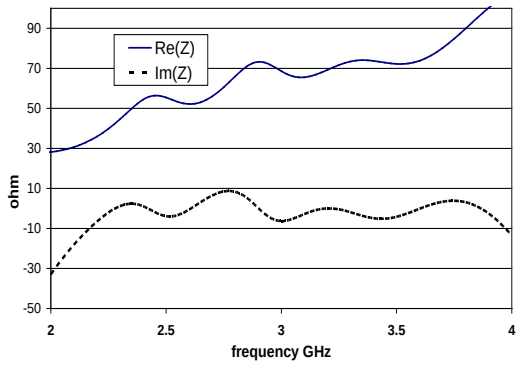

(a)

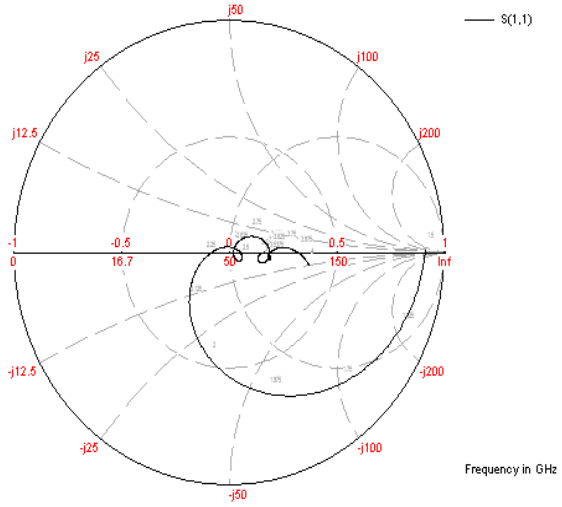

(b)

Fig. 4. (a) Real and Imaginary Parts of Z-Parameters for a pin loaded semi circular patch for β=10^0, (b) the Smith Chart for a pin loaded semicircular patch for β=10^0.

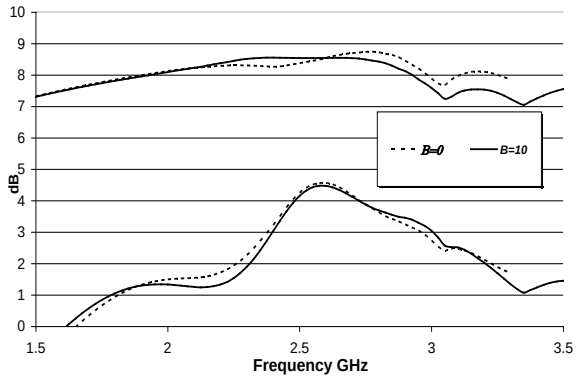

Fig. 5. Maximum directivity, gain versus frequency simulation results for a pin loaded, semicircular patch for β= 0^0, *and 10*°, the parameters are those given in Fig. 3.

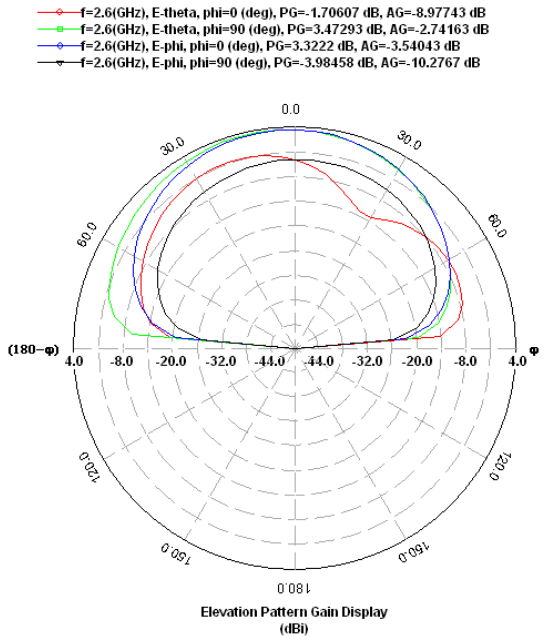

(a) f=2.6 GHz

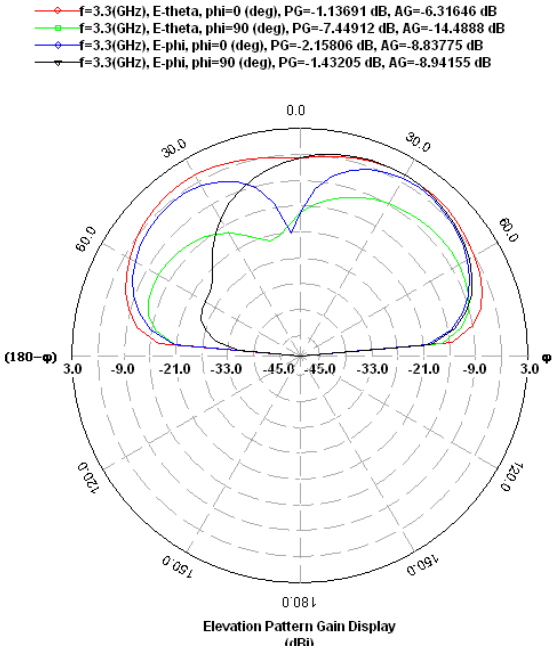

(b) f=3.3 GHz

Fig. 6. The radiation pattern (2D) of E_θ and E_ϕ in the two principal planes ϕ=0 and 90^0 for a pin loaded semi circular patch at (a) f = 2.6 GHz and (b) 3.3 GHz (β=10°).

V. QUARTER CIRCULAR PATCH ANTENNA

As a further reduction of the patch size, a quarter circular patch is considered. The quarter circular patch is shorted at ($r = r_0, \phi = +\alpha$) by a shorting pin as shown in Figure 1(b) Again the feed is placed at ($r_f = r_0, \beta^0$). We have run several simulations with the same patch radius and same pin location as in the case of a half circular patch for easy comparison between the two configurations. The feed position is optimized for maximum impedance bandwidth.

A. Simulation Results for the Quarter-Circular Patch

The Zealand IE3D simulator is used to plot the standing wave ratio for the pin shorted quarter circular patch in Fig. 7. The feed angular position β takes the values 0.10,15,20 and 25^0. From the simulation results, the percentage bandwidths corresponding to SWR$\leq$2 are summarized, along with the center frequency, in Table 2. It is seen that the relative bandwidth obtained when $=10^0$ is about ~29% around the center frequency of 3.04 GHz. Note that the lowest frequency for which SWR=2 is higher for the quarter circular patch; being ~2.7 GHz compared to ~2.1 GHz for the semi-circular patch. A reduction for the lowest frequency end would dictate an increase of the quarter patch radius, which would offset the size reduction to a certain extent. The real and imaginary parts of the input impedance are plotted versus frequency in Fig. 8(a) and the Smith chart representation is given in Fig. 8(b). The resistive component varies between 40 and 100 Ohm and the reactive component varies between -30 and 15 Ohm in the frequency range 2.7-3.7 GHz.

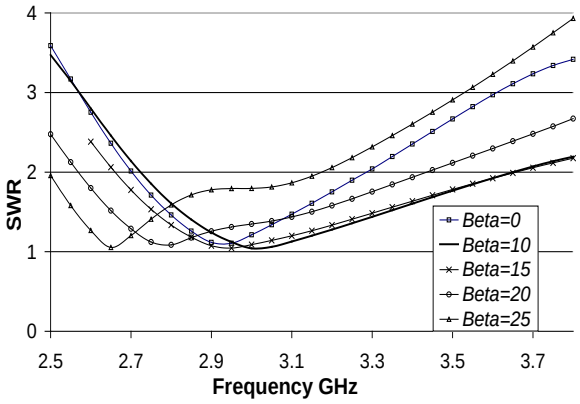

Fig. 7. SWR for a pin loaded quarter circular patch with parameters (in mm): a=35.38, h = 6.28, b = b_f =1.35, $r_o = r_f$ =27.57 mm, α=60°. The feeder angular position β = 0°,10^0,15^0,20^0 and 25^0.

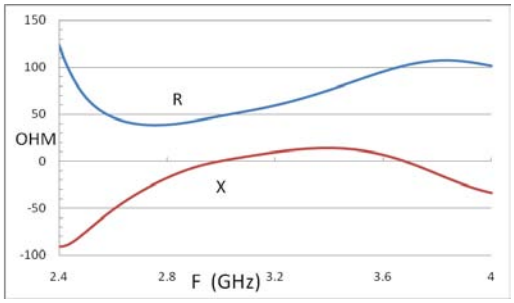

(a)

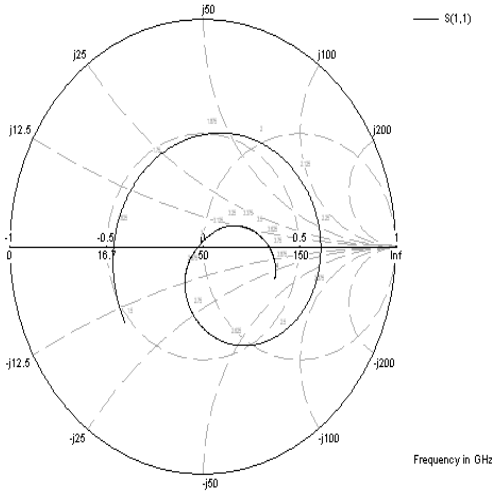

(b)

Fig. 8. (a) Real and Imaginary Parts of input impedance for a pin loaded quarter circular patch for β=10^0, (b) Smith chart representation of the input impedance for a pin loaded quarter circular patch for β=10^0.

B. Directivity, Gain and Radiation Pattern of the Quarter-Circular Patch Antenna

Simulated directivity and gain versus frequency are shown in Fig. 9 for the representative cases of β=0^0 and β=10^0. It is seen that the directivity varies between ~6 dB to 8.3 dB over the band 2.1 to 3.5 GHz. This is a wide range of variation (~2.8 dB) compared to the half patch antenna (~0.5dB). The simulated gain varies between 0 and 5.2 dB over the band 2.1 GHz to 3.5 GHz. Metal losses is expected to be higher for the quarter patch compared to the half circular patch and this accounts for the reduced gain at the lower frequency end. The two dimensional gain patterns at the frequencies GHz are plotted in Fig. 10. As is the case with the semi-circular patch, the radiation is mainly broadside with moderate crosspolar to copolar ratio (-9dB). Low crosspolar radiation is not an important issue in wireless applications.

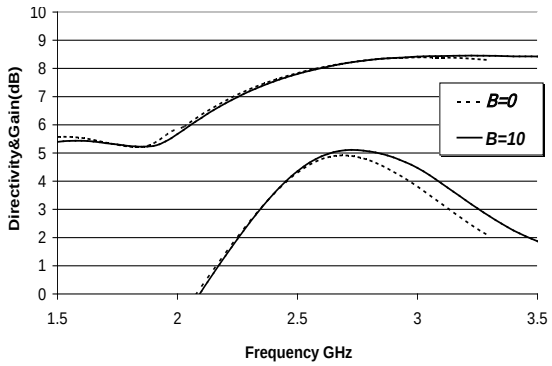

Fig. 9. Maximum directivity, gain versus frequency simulation results for a pin loaded quarter circular patch: $\beta = 0^0$ and 10^0.

VI. Experimental Results

In order to verify the above analytical and simulated designs, a prototype half and quarter circular patch antennas were built on a grounded dielectric substrate. The latter had a relative dielectric constant of 2.2 and thickness= 6.28 mm (made of four layers of 1.57 mm thickness each). The ground plane was a square of dimensions 15x15 cm. The patch geometry was chosen to match the simulated ones for direct comparison with simulation results. In the following, we present the experimental results on both patch geometries.

A. Half Circular Patch Antenna

To perform the measurements, the antenna is connected to the Vector Network Analyzer, Wiltron Model 360B. The measured SWR is shown in Fig. 11. The experimental results demonstrate the operation of the antenna in the range 2.0-4.1 GHz Compared with the simulation results (Fig. 3), a slight shift in the range of operation is noticed (2.1-3.85 GHz in the simulations). This is attributed to several imperfections of connectors, cables substrate permittivity and thickness.

B. Quarter Circular Patch Antenna

The measured SWR for the quarter patch antenna is shown in Fig. 12. The experimental results demonstrate the operation of the antenna in the range 3.1-4.7 GHz compared to 2.75-3.6 GHz in the simulations (Fig. 6). The lowest operating frequency in the measurements is thus shifted to a higher value. However, if the acceptable SWR level can be relaxed to SWR$\leq$2.5 instead of 2, the lower frequency end will be shifted down to 1.7 GHz, giving a substantial increase of the useful bandwidth.

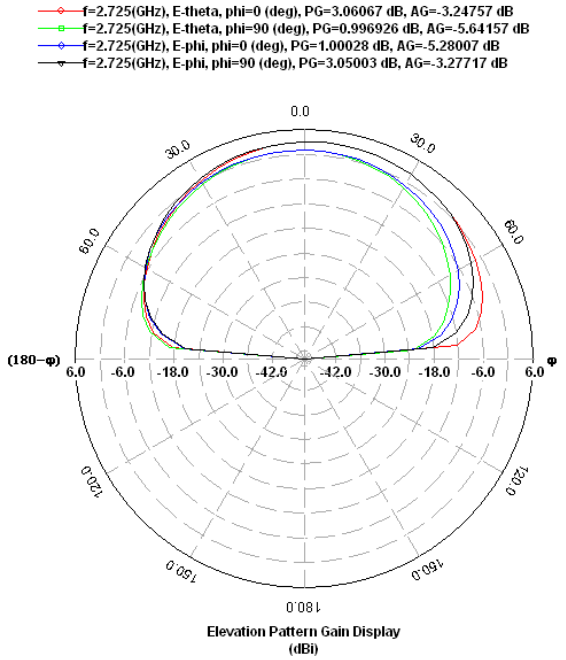

(a)

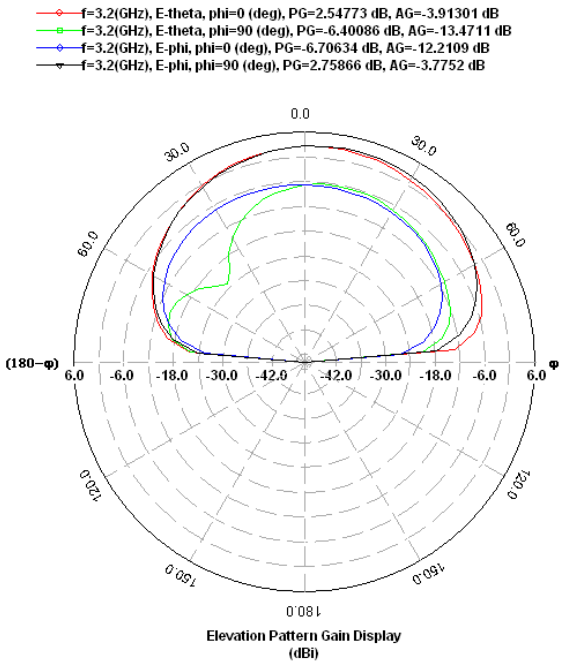

(b)

Fig. 10. The radiation pattern (2D) of E_θ and E_ϕ in the two principal planes ϕ=0 and 90^0 for a pin loaded quarter circular patch for $\beta = 10^0$, (a) at f = 2.6 GHz, (b) f = 3.2 GHz.

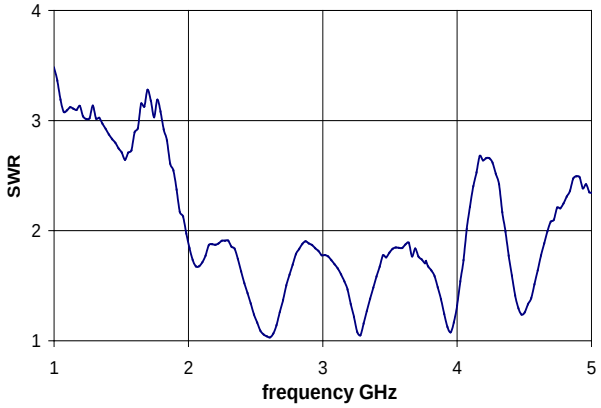

Fig. 11. Experimental result of SWR for semi- circular patch antenna. A broadband operation is achieved over the band 2.0<f <4.1GHz

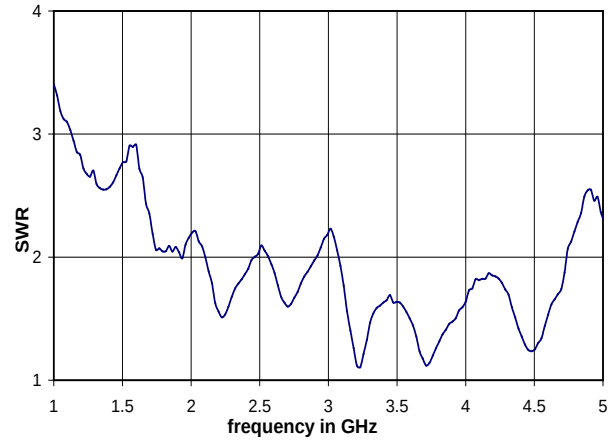

Fig. 12. Experimental result of SWR for quarter circular patch antenna.A broadband operation is achieved over the band 3.1<f <4.7GHz.

VII. Discussions and Conclusions

In an attempt to reach a broadband and compact patch antenna for wireless applications, we have performed theoretical, simulation and experimental work on a pin-loaded half circular and quarter circular patch antennas. The cavity modes of the half circular patch are derived in terms of their resonant frequencies and an initial design of patch geometry for broadband operation is deduced. The design is based on operating the antenna in the band encompassing the resonant frequencies of the second and the third cavity modes. The first mode, having the lowest resonant frequency, can provide a compact, but a narrow band operation as demonstrated earlier in [20, 22] for a full circular shorted patch. Simulation on the Commercial IE3D Zealand software is then used to optimize the feed radius and location for wide band operation.

It is demonstrated that a 58% bandwidth around a center frequency of 2.98 GHz is achievable by using a pin loaded semicircular patch of radius 35.38 mm on an 6.28mm thick substrate of ε_r=2.2. Note that the patch area is merely 13.6% of a free space wavelength squared at 2.5 GHz. The simulated pin loaded quarter circular patch of the same radius gave a 29% bandwidth around the center frequency 3.04 GHz. The patch area is now only 10% of the center wavelength squared. These figures confirm that the broadband operation and antenna compactness are two contradictory requirements. Nevertheless, depending on the application, the attainment of broadband as well as compact antenna designs is possible. The measured results show reasonable agreement with simulated results. For comparison, a conventional circular patch loaded by a chip resistor in [8, p.59-60] is reported to have a 10dB reflection loss bandwidth of only 10.9% and a gain around 4 dBi.

APPENDIX

The aperture field E_z at $r=a$ for a given cavity mode is obtained from equation (2) as,

$$E_z(a,\phi) = \sum_{n=0}^{\infty} [2B_n / \pi ka] \cos n\phi \tag{A1}$$

where B_n is given by equation (7) and E_z above is valid over the surface $|z| \le h$, and $0 \le \phi \le \pi$. This aperture field is equivalent to a ϕ-oriented magnetic current radiating in the outside air region. The radiation fields are obtained by following [20] to get,

$$E_\theta(R,\theta,\phi) = \frac{j\,2h\,e^{-jk_0R}}{\sqrt{\varepsilon_r}\,R} \sum_{n=0}^{\infty} j^n B_n J_n'(k_0 a \sin\theta) \cos n\phi \tag{A2}$$

$$E_\phi(R,\theta,\phi) = \frac{j2h\,e^{-jk_0R}}{\sqrt{\varepsilon_r}\,R} \cos\theta \times \sum_{n=1}^{\infty} j^n B_n n \frac{J_n(k_0 a \sin\theta)}{(k_0 a \sin\theta)} \sin n\phi\,. \tag{A3}$$

In the above (R,θ,ϕ) are spherical coordinates with origin at the projection of the patch center on the ground plane.

REFERENCES

[1] K. R. Carver and J. W. Mink, "Microstrip antenna technology," *IEEE Trans. Antennas Propagat.*, vol. AP-29, no. 1, pp. 2-24, Jan. 1981.

[2] D. M. Pozar and D. H. Schaubert (Eds.), *The Analysis and Design of Microstrip Antennas and Arrays*, IEEE Press, New York, 1996.

[3] R. A. Sainati, *CAD of Microstrip Antenna for Wireless Applications*, Artech House, norwood, MA, 1996.

[4] J. R. James and P. S. Hall, eds, "*Handbook of Microstrip Antennas*," London, UK, Peter Peregrinus, Ltd, ch. 4. 1989.
[5] P. C. Sharma and K. C. Gupta, "Analysis and optimized design of single feed circularly polarized microstrip antennas," *IEEE Trans. Antennas Propagat.*,, vol. 31, no. 6, pp. 949-955, Nov. 1983.
[6] G. Dubost and G. Beauquet, "Linear transmission line model analysis of a circular patch antenna," *Electronic Letters*, vol. 22, pp. 1174-1176, Oct. 1986.
[7] G. Kumar and K. P. Ray, *Broadband Microstrip Antennas*, Artech House, Norwood, MA, 2003.
[8] Kin-Lu Wong, "*Compact and Broadband Microstrip Antennas*," John Wiley, 2002
[9] R. B. Waterhouse, "Small microstrip patch antenna," *Electronics Letters*, vol. 31, no. 8, pp. 604-605, April 1995.
[10] R. B. Waterhouse, S. D. Targonski, and D. M. Kokotoff, "Design and performance of small printed antennas," *IEEE Trans. Antennas Propagat.*, vol. 46, no. 11, pp. 1629-1633, 1998.
[11] S. Dey and R. Mittra, "Compact microstrip patch antenna," *Microwave Optical Technology Letters*, vol. 13, pp. 12-14, Sept. 1996.
[12] K. Wong, C. Tang, and H. T. Chen, "A Compact meandered circular microstrip antenna with a shorting post," *Microwave and Optical Tech. Letters*, vol. 15, no. 3, pp. 147-149, June 1997.
[13] A. F. Sheta, A. Mohra, and S. F. Mahmoud, "A Multi-band operation of compact H-shape microstrip antennas," *Microwave and Optical Technology Letters*, vol. 35, no. 5, pp. 363-367, Dec. 2002.
[14] F. Yang, X. Zhang, X. Ye, and Y. R. Samii, "Wide-band e-shaped patch antennas for wireless communication," *IEEE Trans. Antennas Propagat.*, vol. 49, no. 7, pp. 1088-1100, 2001.
[15] T. Huynh and K. F. Lee, "Single layer single patch wideband microstrip antenna," *Electronics Letters*, vol. 31, pp. 1310-1311, Aug. 1995.
[16] F. Bilotti, M. Manzini, A. Alu, and L. Vegni, "Polygonal patch antennas with reactive impedance surfaces," *Journal of Electromagnetic Waves and Applications (JEMWA*), vol. 20, no. 2, pp. 169-182, 2006.
[17]C. K. Samuel and R. D. Murch, "Compact integrated diversity antenna for wireless communications," *IEEE Trans. Antennas Propagat.*, vol. 49, no. 6, pp. 954-960, June 2001.
[18] K. M. Luck, C. L. Mak, Y. L. Chow, and K. F. Lee, "Broadband microstrip patch antenna," *Electronics Letters*, vol. 34, no. 15, July 1998.
[19] A. A. Eldak, A. Z. Elsherbeni, and C. E. Smith, "Wideband modified bow-tie antenna with single and dual polarization for C and X band applications," *IEEE Trans. Antennas Propagat.*, vol. AP-53, no. 9, pp. 3067-3072, Sept. 2005.
[20] S. F. Mahmoud and R. K. Deeb, "Characteristics of a circular microstrip patch antenna with a shorting post," *Journal of Electromagnetic Waves and Applications (JEMWA*), vol. 16, no. 2, pp. 213-226, 2002.
[21] S. F. Mahmoud and A. F. Almutairi, "A 2-loaded patch as a multiband antenna for wireless communication," *Journal of Applied Computational Electromagnetic Society (ACES)*, pp. 19-25, Nov. 2003.
[22] A. F. Almutairi, S. F. Mahmoud, and N. Aljuhaishi "Wide-Band circular patch antenna with 2-pin loading for wireless communications," *Journal of Electromagnetic Waves and Applications*, JEMWA, vol. 19, no. 6, pp. 839-851, 2005.

Ali Almutairi Received the B.S. degree in electrical engineering from the University of South Florida, Tampa, Florida, in 1993. In December 1993, he has been awarded a full scholarship from Kuwait University to pursue his graduate studies. He received M.S. and Ph.D. degrees in electrical engineering from the University of Florida, Gainesville, Florida, in 1995 and 2000, respectively. At the present, he is the Chairman and an associate professor at Electrical Engineering Department, Kuwait University and director of the Wireless Communication Networks Laboratory. His current research interests include CDMA system, multiuser Detection, cellular networks performance issues, coding and modulation.
Dr. Almutairi is a senior member of IEEE and other professional societies and served as a reviewer for many technical publications.

Nasser. Ahmad Al-Juhaishi was born in 1976. He received the B.S.E. degree of Electrical Engineering in the University of Damascus, Syria in 1999 and the M.S.E. degree in electrical engineering from Kuwait University, Kuwait. His research interests involve ultra wideband electro-magnetics, microwaves, and Antennas.

Samir F. Mahmoud: was graduated from the Electronic Engineering Department, Cairo university, Egypt in 1964. He received the M.Sc and Ph.D. degrees in the Electrical Engineering Department, Queen's university, Kingston, Ontario, Canada in 1970 and 1973. During the academic year 1973-1974, he was a visiting research fellow at the Cooperative Institute for Research in Environmental Sciences (CIRES). Boulder, CO, doing research on Communication in Tunnels. He spent two sabbatical years, 1980-1982, between Queen Mary College, London and the British Aerospace, Stevenage, where he was involved in design of antennas for satellite communication. Currently Dr. Mahmoud is a full professor at the EE Department, Kuwait University. Recently, he has visited several places including Interuniversity Micro-Electronics Centre (IMEC), Leuven, Belgium and spent a sabbatical leave at Queen's University and the Royal Military College, Kingston, Ontario, Canada in 2001-2002. His research activities have been in the areas of antennas, geophysics, tunnel communication, EM wave interaction with composite materials and microwave integrated circuits. Dr. Mahmoud is a Fellow of IET and one of the recipients of the best IEEE/MTT paper for 2003.